

---

## Optimal Design of Model Predictive Control for Voltage and Power Stabilizing in Turbo-Generator System

Mahmoud Elshenawy\*<sup>1</sup>, Helmy Elzoghby<sup>1</sup>, Mohey Bahgat<sup>1</sup>, Abdelghany. M. Abdelghany<sup>2</sup>

<sup>1</sup>Department of Electrical Power and Machines Faculty of Engineering, Helwan University, Cairo, Egypt

<sup>2</sup>on leave for 6 October University, Cairo - Originally Department of Electrical Power and Machines Faculty of Engineering, Helwan University, Cairo, Egypt

---

**Abstract** Power system stability and control requirements have been considerably affected by the steady increase in system interconnections, large rating for individual generating units and high transmission voltage. This paper proposes the model predictive control (MPC) as a powerful control technique to overcome the non-linearity problem of the turbo-generator system. In recent papers, the parameters of the MPC are tuned based on designer experts and trial-error technique which may lead to unacceptable performance. This paper is concerned with the optimal design of the model predictive control (MPC) based on genetic algorithm (GA) and particle swarm optimization (PSO) as enormous optimization techniques. Furthermore, a comparison between the PSO-based MPC, GA-based MPC, and proportional integral (PI) controller based on GA is carried out over a wide range of operating conditions with various fault conditions to emphasize the performance of the proposed techniques.

**Keywords** Model predictive controller (MPC), fractional order PID controller, imperialist competitive algorithm (ICA), genetic algorithm (GA), Turbo-Generator system

---

### Nomenclature

$\delta^{\bullet}$	Rotor Angular Speed
$\delta$	Rotor angle
$H$	Inertia constant
$P_t, Q_t$	Terminal active and reactive power at infinite bus bar
$V_{fd}$	Field voltage
$V_t$	Terminal voltage
$V_b$	Infinite- bus bar voltage
$\Psi_f$	Field flux linkage
$\Psi_d, \Psi_q$	d-axis and q-axis stator flux linkages
$\Psi_{kd}, \Psi_{kq}$	d-axis and q-axis damper winding flux linkages
$I_d, I_q$	d-axis and q-axis stator currents
$I_{kd}, I_{kq}$	d-axis and q-axis damper winding currents
$X_f$	Self-reactance of field winding
$X_d, X_q$	Synchronous reactance in d-axis and q- axis circuit
$X_{kd}, X_{kq}$	Self-reactance in d-axis and q-axis of the damper winding
$X_{ad}$	Reactance between armature and field winding



$X_e$	Transformer and line reactance
$R_e$	Transformer and line resistance
$R_a$	Stator resistance
$R_f$	Field resistance
$R_{kd}, R_{kq}$	Resistance of d-axis and q.-axis damper winding
$V_d, V_q$	Stator voltage in d-axis and q-axis
$V_{kd}, V_{kq}$	Damper winding voltage in d-and q- axis circuits
$\Delta ( )$	Denoting incremental quantity
$p ( )$	The operator { d/dt }
$\omega_o$	Angular frequency of infinite bus bar
$\omega$	Angular frequency of the rotor
$T_e$	The electric torque
$T_m$	Mechanical Torque of generator shaft
$\mu_{hp}$	Steam flow of high pressure
$\mu_{rh}$	Steam flow of reheater
$\mu_{ip}$	Steam flow of intermediate pressure
$\mu_l$	Steam flow of low pressure
$\mu_g$	Governor and interceptor valve positions
$\tau_{lp}$	Time constant of low pressure stage
$\tau_{ip}$	Time constant of intermediate pressure stage
$\tau_{rh}$	Time constant of reheater
$\tau_{hp}$	Time constant of high pressure stage
$\tau_{iv}$	Time constant of interceptor valve
$\tau_{mv}$	Time constant of main valve
$P_o$	Boiler steam pressure
$F_{hp}$	Power fraction from high pressure stage
$F_{ip}$	Power fraction from intermediate stage
$F_{lp}$	Power fraction from low pressure stage

## 1. Introduction

The increasing complexity of modern power systems, with high transmission voltages, long distance transmission, complex interconnections and large rating for individual generating units, has prompted a substantial effort towards the development of improved methods of operation and control. The effectiveness of controllers has been facilitated by recent developments in technology, such as fast turbine valving [1], fast acting circuit breakers and thyristor excitation systems [2]. Fast excitation systems have allowed controllers to be considered which force a rapid change of field voltage in either direction, and therefore rotor oscillations due to disturbances are quickly damped. The advent of electro-hydraulic governors with fast turbine valving, giving simultaneous operation of the inlet and intercept valves, has considerably altered the concepts of turbine control [3]. In recent, there are several approaches applied to improve the transient stability of turbo-generators. In [4], the state-variable feedback control is utilizing to improve the transient stability of turbo-generators. In some cases, only the excitation was controlled, and in others, both excitation and turbine input power are controlled. The nonlinear system equations of the turbo-generator system are linearized at a specific operating condition, and linear optimal control theory is used to calculate the feedback gains of the digital controller. The use of linear control theory based on accurate reduced-order linear models of turbo-generator dynamics is presented in [5-7]. In these papers, the models have been estimated using system identification. The first group has used the state formulation to identify the turbo-generator by linearized models. The other group formulated these models using output prediction equation, employing output variables only. Accordingly, the optimal controller gains



have been calculated using the linear control theory [8-11]. All these techniques fail to give an acceptable response due to the nonlinearity of the system. In [10-12], several methods have been suggested to obtain reasonable solutions to this problem. One of these solutions for the nonlinearity problem of the turbo-generator is adaptive model following control of generator terminal voltage. The basic idea of such methods is to state definitely, by means of an effectively realized model, the desired behavior of the closed-loop system. Automatic adjustment of the controller gains is then carried out in such a way that the behavior error between the outputs of the desired behavior model and those of the close-loop system is made as small as possible. The use of this approach improves the steady-state and transient stability for the generator. It will be known that the adaptive controller gains calculation depends on several mathematical treatments takes very long time. In addition, these controller gains highly depend upon the turbo-generator parameters which may be lack calculated. For the previous problems of these control approaches, the model predictive control is being facilitated for the following reasons: this technique is very simple as they depend on the input/output values only regardless to the nonlinearity of the system, mathematical equations or system parameters [12-17]. However, the prediction horizon, control horizon, sample time, control weight factor MPC need a proper tuning to get a good performance by the controller. The objective of this work is to describe the theory, design, and test of two practical solutions to overcome the nonlinearity problem of the turbo-generator system. The first one is the MPC based on the genetic algorithm (GA) approach. The second is the MPC based on the particle swarm optimization (PSO) approach. These approaches depend on iterative and finite horizon optimization of a plant model, easiness of implementation and operating. Furthermore, incorporated transport short circuit and mechanical and electrical variation are considered. A Comparison between PSO-based MPC, GA-based MPC and proportional integral (PI) controller has proved the superiority of the proposed design in capturing system nonlinearities and transport short circuit and mechanical and electrical variation. Consequently, the system stability test under increased load perturbations and excessive short circuit and mechanical and electrical variation is considered. In addition, the robustness test of the proposed design against system parameters uncertainties is carried.

## 2. System Modeling and Description

Turbo-generators are highly nonlinear, fast acting, multivariable systems with dynamic characteristics that vary as operating conditions change [24].

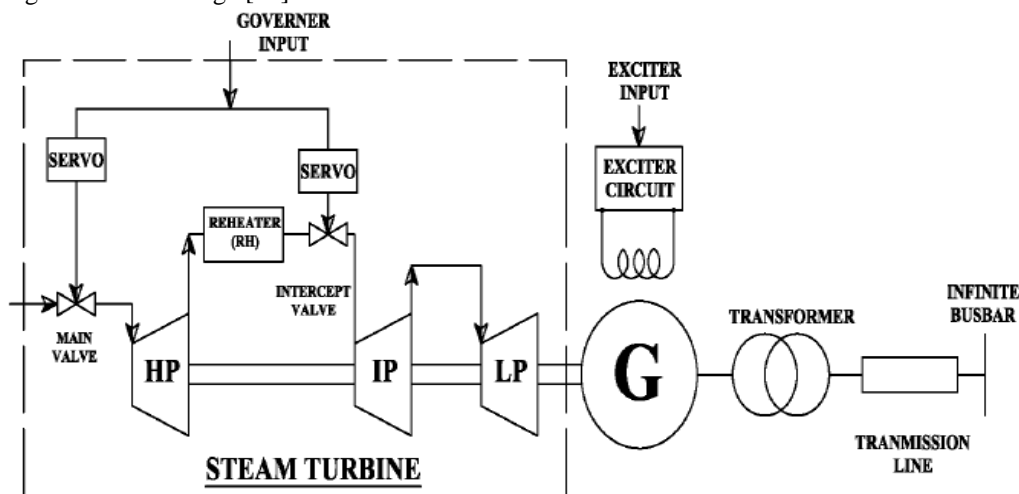


Figure 1: Schematic diagram of Turbo-Generator System.

As a result, the generator terminal voltage and terminal power have to be adjusted to reach the optimum requirements of the power system. Effective control of turbo-generators is important, since these machines are responsible for ensuring the stability and security of the electric power grid. Automatic voltage regulator (AVR) and turbine governor valve position are designed using linearized models. Optimal and adaptive controllers for the generator exciter and turbine governor, designed to control the turbo-generator and turbine performance during disturbances, may be applied to the turbo-generator system. Also the controllers will extend the transient and steady state stability boundaries. The system considered in this study consists of a turbo-generator unit



connected to the infinite busbar through a transformer and transmission system comprising two transmission lines in parallel [25]. Fig.1. shows the schematic diagram of the turbo-generator system.

The equations of the non- linear model of synchronous generator can be expressed in state-space form as follows [25]:

$$\dot{S} = f(s, u), \text{ where } u = E_{fd}$$

The state vector (S) is:

$$S = [ \delta \ p\delta \ \psi_{fd} \ \psi_d \ \psi_{kd} \ \psi_q \ \psi_{kq} ] \quad (1)$$

And

$$pS_1 = S_2 \quad (2)$$

$$pS_2 = C_1 T_m + S_4(C_2 S_6 + C_3 S_7) + S_6(C_4 S_3 + C_5 S_5) + C_6 S_2 \quad (3)$$

$$pS_3 = C_7 E_{fd} + C_8 S_3 + C_9 S_4 + C_{10} S_5 \quad (4)$$

$$pS_4 = C_{11} \sin(S_1) + C_{12} S_3 + C_{13} S_4 + C_{14} S_5 + S_6 + S_2 S_6 \quad (5)$$

$$pS_5 = C_{15} S_3 + C_{16} S_4 + C_{17} S_5 \quad (6)$$

$$pS_6 = C_{11} \cos(S_1) + C_{18} S_6 + C_{19} S_7 - \omega_o S_4 - S_2 S_4 \quad (7)$$

$$pS_7 = C_{20} S_6 + C_{21} S_7 \quad (8)$$

The state vector of the state-space model of a steam turbine is:

$$[S_8 S_9 S_{10} S_{11} S_{12} S_{13}]^T = [\mu_{hp} \mu_{rh} \mu_{ip} \mu_{ip} Y_{mv} Y_{iv}]^T \quad (9)$$

And

$$P\mu_{hp} = (P_o Y_{mv} - \mu_{hp}) / \tau_{hp} \quad (10)$$

$$P\mu_{rh} = (\mu_{hp} - \mu_{rh}) / \tau_{rh} \quad (11)$$

$$\mu_{ip} = (\mu_{rh} Y_{iv} - \mu_{ip}) / \tau_{ip} \quad (12)$$

$$P\mu_{ip} = (\mu_{ip} - \mu_{ip}) / \tau_{ip} \quad (13)$$

$$P Y_{mv} = (\mu_g - Y_{mv}) / \tau_{mv} \quad (14)$$

$$P Y_{iv} = (\mu_g - Y_{iv}) / \tau_{iv} \quad (15)$$

$$T_m = F_{hp} \mu_{hp} + F_{ip} \mu_{ip} + F_{lp} \mu_{lp} \quad (16)$$

The thirteen order nonlinear turbo-generator model is defined by combining the equations 2 to 8 as a representative of the generator and equations 10 to 15 as a representative of the steam turbine.

And the electric equations are:

$$V_{td} = V_b \sin(\delta) + R_e I_d - X_e I_q \quad (17)$$

$$V_{tq} = V_b \cos(\delta) + R_e I_q + X_e I_d \quad (18)$$

$$V_t^2 = V_{td}^2 + V_{tq}^2 \quad (19)$$

$$I_t^2 = I_d^2 + I_q^2 \quad (20)$$

$$P_t = V_{td} I_d + V_{tq} I_q \quad (21)$$

And the direct current equations are:

$$\begin{bmatrix} I_{fd} \\ I_d \\ I_{kd} \end{bmatrix} = \begin{bmatrix} Y_{11} & Y_{12} & Y_{13} \\ Y_{21} & Y_{22} & Y_{23} \\ Y_{31} & Y_{32} & Y_{33} \end{bmatrix}^{-1} \begin{bmatrix} \Psi_{fd} \\ \Psi_d \\ \Psi_{kd} \end{bmatrix} \quad (22)$$

And the quadrature current equations are:

$$\begin{bmatrix} I_q \\ I_{kq} \end{bmatrix} = \begin{bmatrix} D_{11} & D_{12} \\ D_{21} & D_{22} \end{bmatrix}^{-1} \begin{bmatrix} \Psi_q \\ \Psi_{kq} \end{bmatrix} \quad (23)$$

All constants are defined in the Appendices.

### 3. Theory of MPC

The MPC has demonstrated to effectively control an extensive variety of utilization in industry, for example, chemical process, oil industry, electro-mechanical applications and numerous different systems [16, 17]. The MPC control strategy depends on an explicit utilization of an expectation model of the system reaction to get the control actions in order to minimize an objective function. The objective of the optimization incorporates the



minimization of the contrast between the predicted output and the reference signal, and the control action subjected to recommended requirements. The viability of the MPC is shown to be equal to the optimal control [16]. It shows its principle quality in its computational convenience, practical applications, compensation for time delays, treatment of limitations, and potential for future augmentations of the technique. At each control step, the principal contribution to the optimal arrangement is sent into the plant, and the whole estimation is repeated at resulting control steps. The reason for taking new estimations at each time step is to overcome the unmeasured disturbances and the inaccuracy of model, both of which cause the plant output to be not quite the same as the predicted output [17]. The control operations at each prediction step are shown in Figure 2.

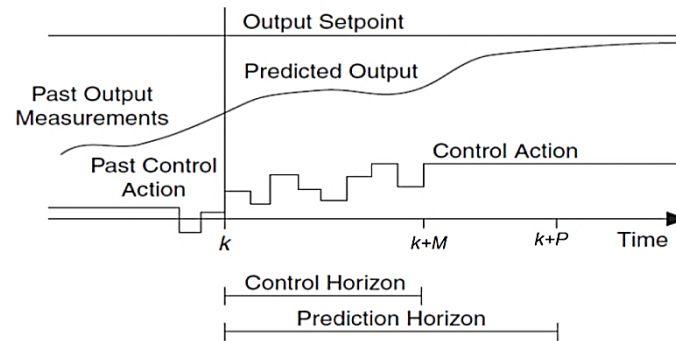


Figure 2: Basic concept for Model Predictive Control.

The operation of MPC is carried out at the  $k$ -th sampling instant. The sampling takes this form  $0, T_s, 2T_s, 3T_s, \dots, kT_s$ , when the MPC starts at time  $t=0$ . Where,  $T_s$  is the sample time and  $K$  is the current sample. The predicted control signal and the predicted output is founded based on the minimizing of the following objective function,

$$\text{Min}_{u_k, \dots, u_{k+p-1}} \sum_{i=1}^P [Q(r_{k+i} - \hat{y}_{k+i})^2 + R(\Delta u_{k+i-1})^2] \quad (24)$$

Such that,

$$u_{\min} \leq u_{k+i} \leq u_{\max}$$

$$y_{\min} \leq \hat{y}_{k+i} \leq y_{\max}$$

$$|\Delta u_{k+i}| \leq \Delta u_{\max}$$

Where  $\Delta u_j = u_j - u_{j-1}$  is the adjustment at sampling instant  $j$ , and  $Q$  and  $R$  are non-negative weights. The Values of set points, measured disturbances, and constraints are specified over a finite horizon of future sampling instants  $k+1, k+2, \dots, k+P$ , where  $P$  is the prediction horizon and a finite integer  $\geq 1$  as shown in Fig. 2. The MPC computes the  $M$  moves  $u(k), u(k+1), \dots, u(k+M-1)$ , where  $M$  is the control horizon and  $1 \leq M \leq P$ .

Each MPC require a proper adjustment of the  $T_s, Q, R, M,$  and  $P$  to give an acceptable performance so this paper proposes the PSO and the GA for the optimal tuning of MPC parameters.

#### 4. Particle Swarm Optimization Algorithm

The particle swarm optimization (PSO) strategy has been observed to be robust in solving complicated optimization problems [18-23]. It can solve the problems which contain nonlinearity. Furthermore, it can deal with the non-differentiability problems and the problems which contain various optima. This method is developed from research on swarm such as fish schooling and bird flocking. The implementation of it is easy with efficient computation. In addition, the convergence characteristic of it is stable. Rather than utilizing developmental administrators to update the particle (individual), like in other transformative computational algorithms, every particle in PSO flies in the inquiry space with the velocity which progressively adjusted by its own flying experience and its companions' flying experience. Each particle is regarded as a volume less particle in dimensional search space. Every particle monitors its directions in the problem space, which are related with the best arrangement (objective value). It has reached very far and this value is called  $P_{\text{best}}$ . Another best value that is followed by the global variant of the particle swarm enhancer is the general best value, and its place,



acquired so far by any particle in the gathering, is called  $g_{best}$ . The PSO idea comprises it at each time step, varying the velocity of each particle toward its  $P_{best}$  and  $g_{best}$  places. Speeding up is weighted by an arbitrary term, with partitioned irregular numbers being created for increasing speed toward  $P_{best}$  and  $g_{best}$  places.

For example, the  $j$  th particle is act as  $X_j=(X_{j,1}, X_{j,2}, \dots, X_{j,g})$  in the  $g$ -dimensional space. The best previous location of the  $j$ th particle is recorded and represented as,  $P_{bestj}=( P_{bestj,1}, P_{bestj,2}, \dots, P_{bestj,g})$ . The index of the best particle between all of the particles in the gathering acts as the  $g_{bestj}$ . The rate of the position change (velocity) for particle  $j$  acts as,

$V_j=(V_{j,1}, V_{j,2}, \dots, V_{j,g})$ . The modified velocity and position of every particle can be determined by using the present velocity and the distance from  $P_{bestj,g}$  to  $g_{bestj}$  as shown in the following formulas:

$$V_j^{(t+1)} = W * V_{j,g}^{(t)} + C_1 * rand * (P_{bestj,g} - X_{j,g}^{(t)}) + C_2 * rand * (g_{bestj} - X_{j,g}^{(t)}) \tag{25}$$

$$X_{j,g}^{(t+1)} = X_{j,g}^{(t)} + V_{j,g}^{(t+1)} \tag{26}$$

$j=1, 2, \dots, n$  and  $g=1, 2, \dots, m$

Where

- $n$  number of particles in a group
- $m$  number of members in a particle
- $t$  pointer of iterations (generations)
- $V_{j,g}^{(t)}$  velocity of particle at iteration,  
 $V_g^{min} \leq V_{j,g}^{(t)} \leq V_g^{max}$
- $W$  inertia weight factor
- $C_1, C_2$  acceleration constant
- $rand$  random number between 0 and 1
- $X_{j,g}^{(t)}$  current position of particle at iteration
- $P_{bestj,g}$   $P_{best}$  of particle  $j$
- $g_{bestj}$   $g_{best}$  of the group

The suitable choice of  $W$  gives a balance amongst global and local investigations, in this manner requiring less iteration on average to discover an adequately optimal solution. As initially developed,  $W$  frequently decreases linearly from around 0.9 to 0.4 through a run. Always, the inertia weight  $W$  is calculated from the following equation:

$$w = w_{max} - \frac{w_{max} - w_{min}}{iter_{max}} * iter \tag{27}$$

Where  $iter_{max}$  is the maximum number of iterations and  $iter$  is the present number of iterations. The flowchart of PSO is shown in Figure: 3.

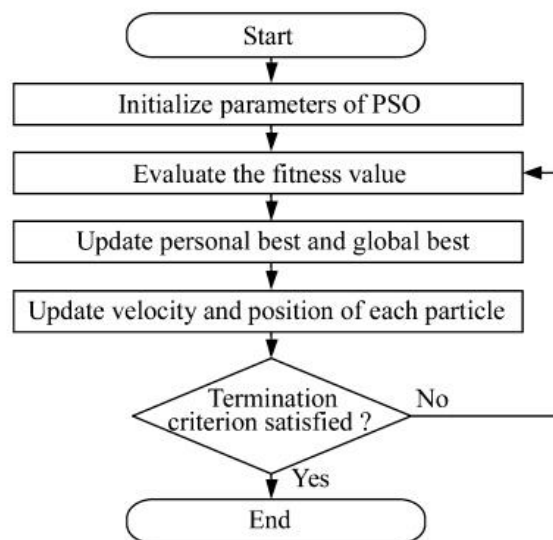


Figure 3: The flowchart of PSO



**5. Turbo-Generator System based on MPC**

In the proposed turbo-generator system [25] there are two MPC controller required to control the voltage and the power of the generator as shown in Figure: 4.

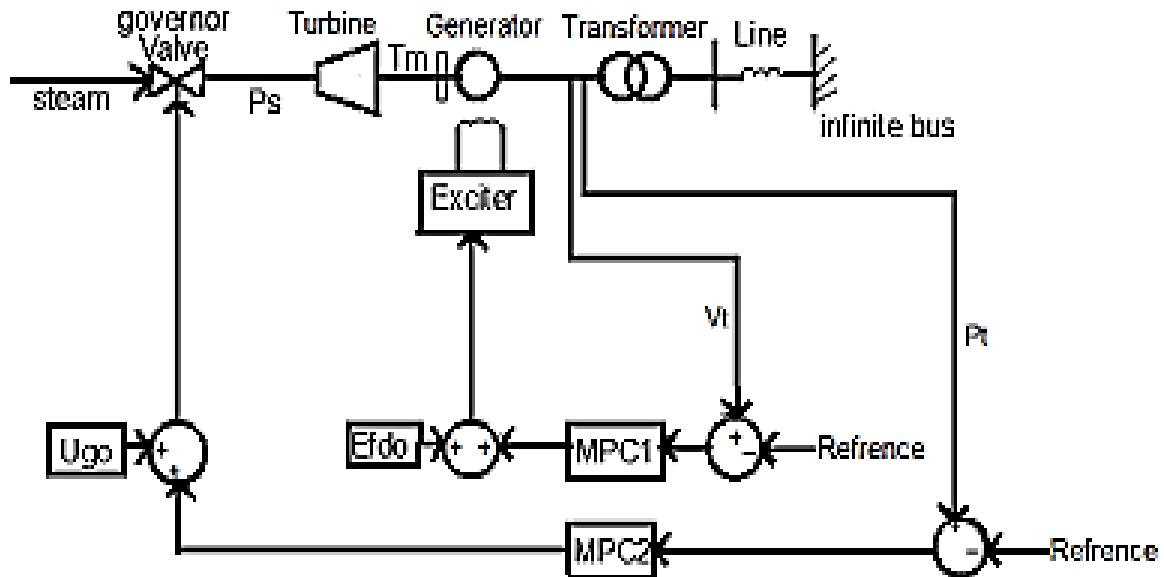


Figure 4: Turbo-generator system controlled by MPC

The proposed configuration is done in Matlab Simulink utilizing MPC toolbox. The configuration is started by determining the linear time invariant (LTI) model of the plant to be controlled. These LTI models act as discrete state-space models. The PSO and GA are devoted for searching the MPC parameters in order to minimize the following objective function:

$$J = \int_{t=0}^{t=t_f} t [ |V_{ref} - V_t(t)| + |P_{ref} - P_t| ] \tag{28}$$

The optimal parameters of GA-based PI controller, GA-based MPC, PSO-based MPC are listed in Table 1 where the corresponding objective functions are computed.

**Table 1:** Controller parameters and the objective function (J)

	PSO-based MPC	GA-based MPC	GA-based PI
<b>MPC<sub>1</sub> parameters</b>	T <sub>s1</sub> = 0.769, P <sub>1</sub> = 29, M <sub>1</sub> = 29	T <sub>s1</sub> = 1.622, P <sub>1</sub> = 184, M <sub>1</sub> = 52	K <sub>p1</sub> =0.01 K <sub>i1</sub> =12
<b>MPC<sub>2</sub> parameters</b>	r <sub>1</sub> = 0.689, q <sub>1</sub> = 0.1 T <sub>s2</sub> = 0.468, P <sub>2</sub> = 118 M <sub>2</sub> = 100 R <sub>2</sub> = 0.007, q <sub>2</sub> = 4.57	r <sub>1</sub> = 0.6490, q <sub>1</sub> = 7.8640 T <sub>s2</sub> = 0.5060, P <sub>2</sub> = 92, M <sub>2</sub> = 20 R <sub>2</sub> = 0.116, q <sub>2</sub> =3.515	K <sub>p2</sub> =0.8 K <sub>i2</sub> =9
<b>Objective function (J)</b>	0.9115	2.0969	5.11

From Table 1, it is clear that the value of J in the case of PSO-based MPC is the minimum objective value.

**6. Simulation Results**

In this section, the simulations are carried out to study the dynamic response of a single machine infinite bus power system with GA-based PI controller, GA-based MPC, and PSO-based MPC. To exhibit the validity of the proposed configuration, tests such as terminal voltage and output power regulation, attenuation of exogenous disturbance represented by symmetrical three phase short circuit and mechanical and electrical variation for the studied system are carried out. Furthermore, the robustness test of the proposed design against system parameters uncertainties is carried.

**6.1 Effect of Three Phase Short Circuit Disturbance with 120ms Fault Time**

This test is provided to show the feasibility of designed MPC in attenuating heavy exogenous disturbance represented by three phase short circuit that is applied at the infinite bus and lasting for 120 milliseconds. In the

beginning, the nonlinear model of a single machine infinite bus power system reference values is set to  $V_{ref} = 1.064$  p.u and  $P_{ref} = 0.8$  p.u. Once the system has settled down to its steady state, a 120-ms balanced three phase short circuit is applied ( $t = 1$ s) at the terminal of the machine. Figure 5 shows the system time response of the system terminal voltage and power driven by GA-PI and GA-MPC and Swarm-MPC. As shown in Figure 5, oscillations are presented in  $V_t$  and  $P_t$ , the system regains its stability after a few seconds. It is clear that the PSO-based MPC has the best performance summarized in faster response (2 s for PSO- based MPC, 4 s for GA-based MPC and 6 s for GA-based PI controller) and fewer oscillations than GA-based PI and GA-based MPC.

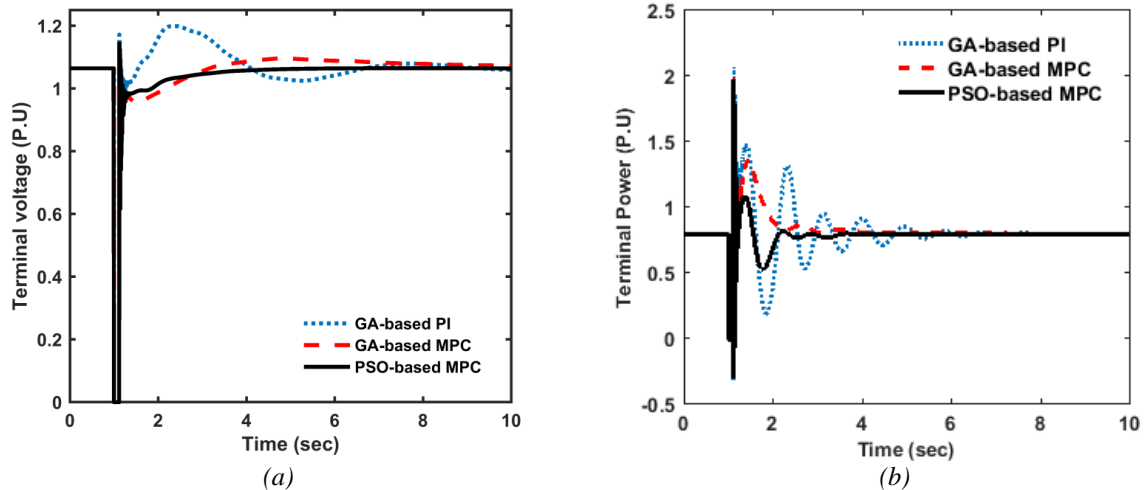


Figure 5: Effect of three phase short circuit disturbance with  $t_f = 120$ ms (a) Voltage terminal response, (b) Power terminal response

## 6.2 Effect of Three Phase Short Circuit Disturbance with 260ms Fault Time

This test is carried out to show the performance of MPC in case of increasing the three phase short circuit duration that is applied at the infinite bus and lasting for 260 milliseconds. As shown in Figure 6, the oscillations are presented in  $V_t$  and  $P_t$ , the system regains its stability after a few seconds. It is clear that PSO-based MPC show improved performance summarized in faster response (4 s for PSO- based MPC, 6 s for GA-based MPC and 9 s for GA-based PI controller) with fewer oscillations than GA-based PI controller and GA-based MPC.

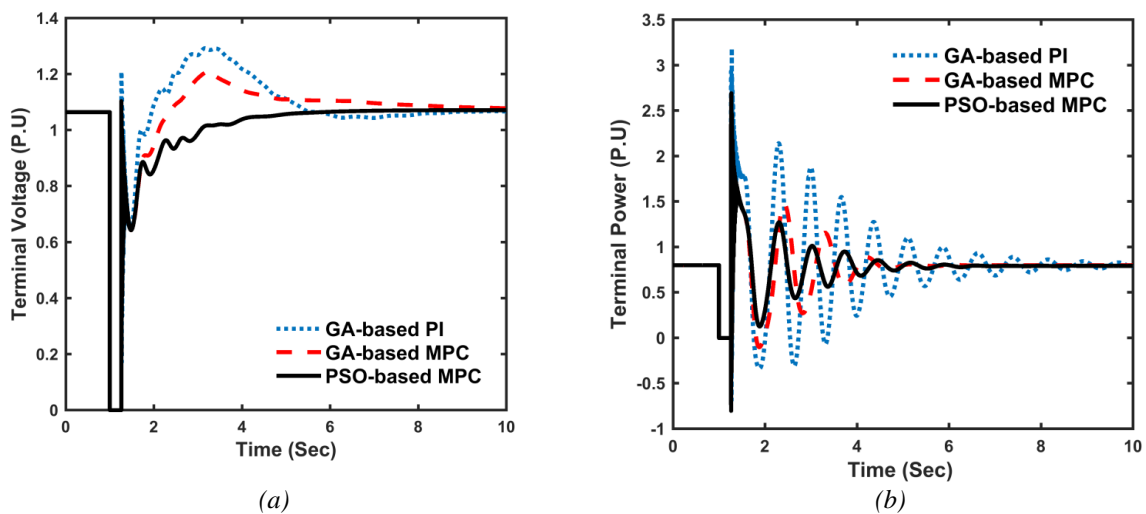


Figure 6: Effect of three phase short circuit disturbance with  $t_f = 200$ ms (a) Voltage terminal response, (b) Power terminal response



### 6.3 Effect of Load Variation By 15% Increase with 120ms Fault Time

In this test, a 15% increase in voltage with 120ms disturbance time is applied. As shown in Figure 7, oscillations are presented in  $V_t$  and  $P_t$ , the system regains its stability after a few seconds. It is clear that the system response with PSO-based MPC more damped and faster response (2 s for PSO- based MPC, 4s for GA-MPC and 6s for GA-PI) than GA-based MPC and GA-based PI controller.

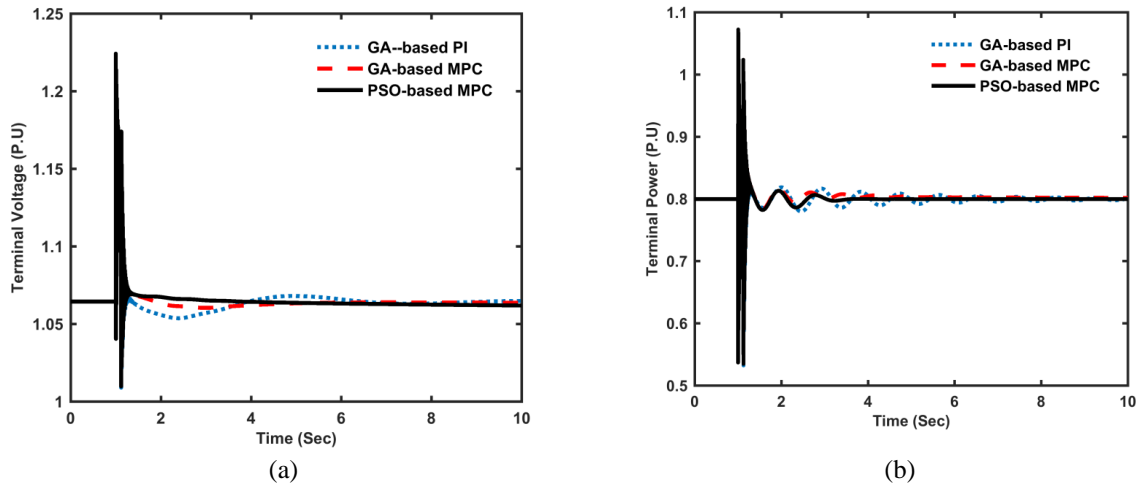


Figure 7: Effect of load variation by 15% increase with  $t_d= 120ms$  (a) Voltage terminal response, (b) Power terminal response.

### 6.4 Effect of Mechanical Power Variation by 15% Decrease with 120ms Fault Time

In this test, a 15% decrease in mechanical input with 120ms disturbance time is applied. As shown in Figure 8, oscillations are presented in  $V_t$  and  $P_t$ , the system regains its stability after a few seconds. It is clear that PSO-based MPC show improved performance summarized in faster response (2.5 s for PSO- based MPC, 5 s for GA-MPC and 7 s for GA-PI) with fewer oscillations than GA-based PI controller and GA-based MPC.

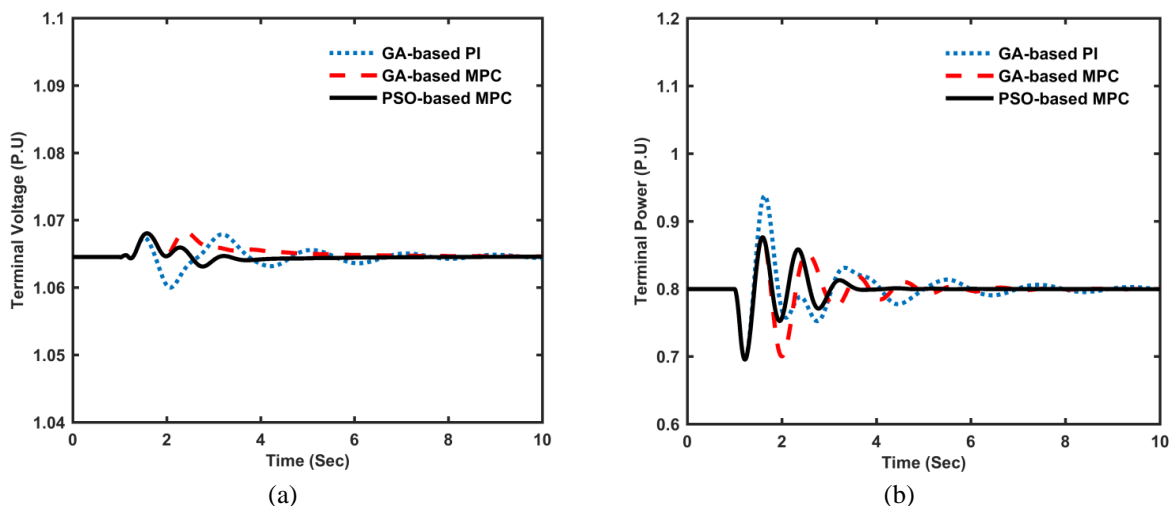


Figure 8: Effect of mechanical power variation by 15% decrease with 120ms (a) Voltage terminal response, (b) Power terminal response

### 6.5 Effect of Mechanical Power Variation by 15% Increase and Voltage Variation by 15% Decrease with 120ms

In this test a 15% increase in mechanical power and 15% decrease in voltage with 120ms fault time are applied. As shown in Figure 9, oscillations are presented in  $V_t$  and  $P_t$ , the system regains its stability after a few seconds. It is clear that MPC show improved performance summarized in faster response (2.5 s for PSO- based MPC, 5 s for GA-MPC and 7 s for GA-PI) with fewer oscillations than GA-PI and GA- MPC.



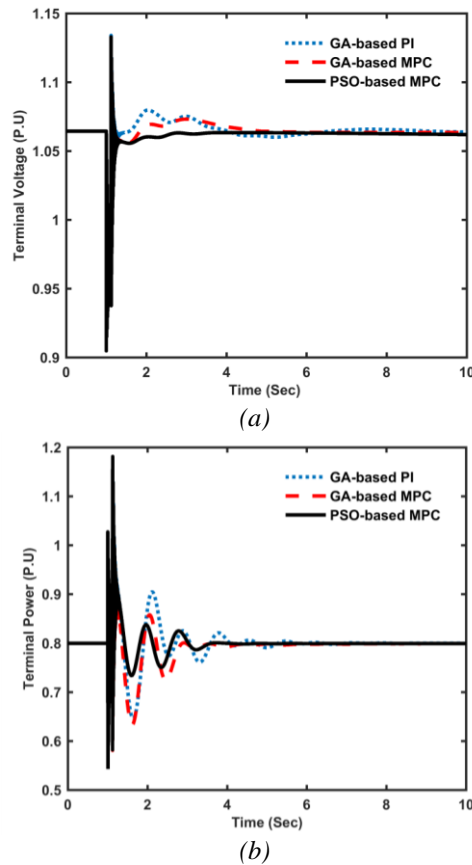
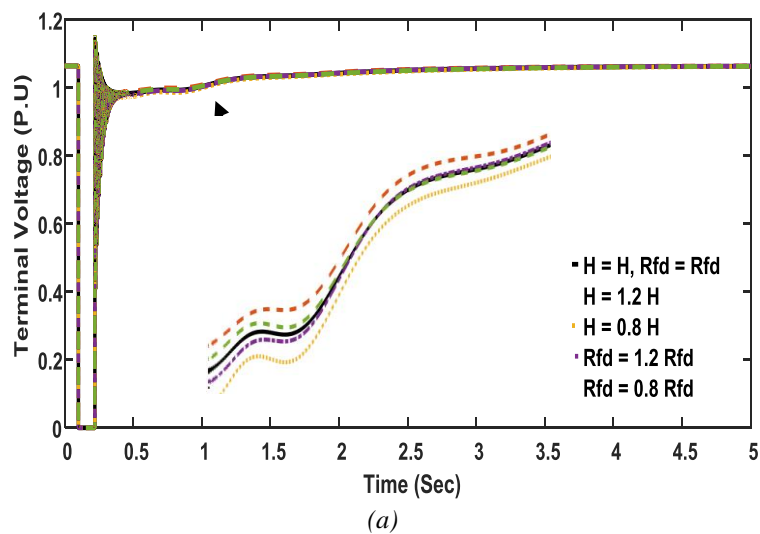


Figure 9: Effect of mechanical power input variation by 15% increase and load variation by 15% decrease with  $t_d = 120ms$  (a) Voltage terminal response, (b) Power terminal response

**6.6 Robustness study**

Robustness of the proposed PSO-based MPC design against system parameter uncertainties is implemented for further testing. To carry out this test, the inertia and field resistance coefficient are assumed to be uncertain and vary around its nominal value ( $H, R_{fd}$ ) by  $\pm 20\%$ , i.e.  $(H, R_{fd}) \in [(0.2(H, R_{fd}), 1.2(H, R_{fd}))]$ . The nonlinear model of the system is stimulated at the nominal, upper and lower limits of  $(H, R_{fd})$  to confirm the robustness of the proposed design. As shown in Figure 10, the proposed PSO-based MPC can damp the system oscillation under system uncertainties with a non-significant change in the system response.



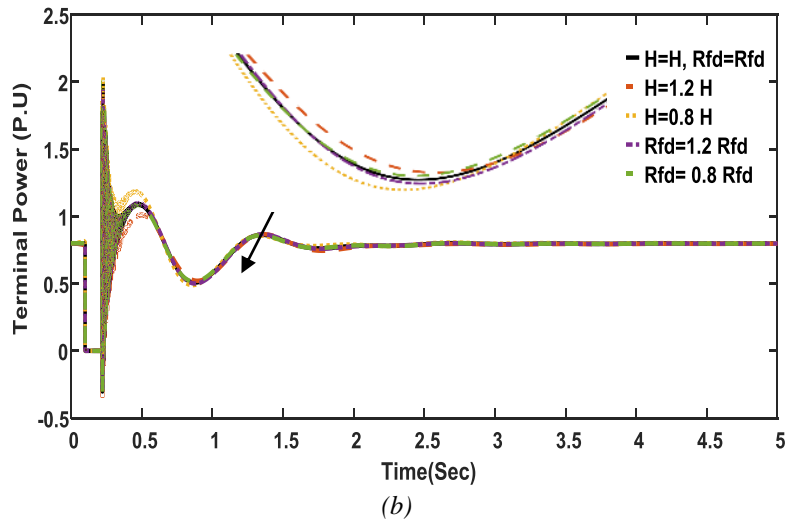


Figure 10: System Response Subject to Robustness Study (a) Voltage terminal response, (b) Power terminal response.

## 7. Conclusion

In this paper, the parameters of model predictive control in Turbo-generator system are tuned by PSO algorithm and GA PSO algorithm to cope with system nonlinearities comprising exciter and governor Turbo-generator system. Furthermore, incorporated transport short circuit and mechanical and electrical variation are considered. A candidate time-domain based objective function has been considered to minimize both maximum overshooting and settling time. Comparing the proposed PSO-based MPC to GA-based MPC and GA-based PI controllers has proved the superiority of PSO-based MPC design in capturing system nonlinearities and transport short circuit and mechanical and electrical variation. Consequently, the suggested design can guarantee system stability under increased load perturbations and excessive short circuit and mechanical and electrical variation. Simulation results have been carried out to emphasize on the robustness of the proposed design against system parameters uncertainties.

## Appendix

$\omega_o=400*\text{atan}(1)$ ;  $H=3.25$ ;  $R_{fd}=1.5*0.0015$ ;  $R_{kd}=0.038$ ;  $X_{ad}=1.86$ ;  $X_{aq}=1.77$ ;  $X_{fd}=1.97$ ;  $X_d=2$ ;  $X_q=1.91$ ;  $X_{kd}=1.936$ ;  $X_{kq}=1.9$ ;  $K_d=0$ ;  $X_i=0.101$ ;  $R_l=0.0025/2$ ;  $X_l=0.352/2$ ;  $R_a=0.005$ ;  $R_f=0$ ;  $R_e=0$ ;  $R_e=0$ ;  $X_e=X_l+X_p$ ;  $K=0$ ;  $F_{hp}=0.24$ ;  $F_{ip}=0.34$ ;  $F_{lp}=0.42$ ;  $P_0=1.2$ ;  $X_{fkd}=X_{ad}$ ;  $X_{akd}=X_{ad}$ ;  $X_{akq}=X_{aq}$ ;  $T_{mv}=0.1$ ;  $T_{iv}=0.1$ ;  $T_{hp}=0.3$ ;  $T_{rh}=1$ ;  $T_{ip}=0.3$ ;  $T_{lp}=0.72$ ;  $F_{hp}=0.24$ ;  $F_{ip}=0.34$ ;  $F_{lp}=0.42$ ;  $\omega = \omega_o$ ;

$A=[X_{fd} \ -X_{ad}X_{ad}; X_{ad} \ -X_dX_{ad}; X_{ad} \ -X_{ad}X_{kd}]$ ;  $Y=\text{inv}(A)$ ;

$B=[-X_qX_{aq}; -X_{aq}X_{kq}]$ ;  $D=\text{inv}(B)$ ;

$c_1=\omega_o/(2*H)$ ;  $d_{11}=D(1,1)$ ;  $Y_{22}=Y(2,2)$ ;  $c_2=c_1*(Y_{22}-d_{11})$ ;  $d_{12}=D(1,2)$ ;  $c_3=c_1*d_{12}$ ;  $Y_{21}=Y(2,1)$ ;  $c_4=c_1*Y_{21}$ ;  $Y_{23}=Y(2,3)$ ;  $c_5=c_1*Y_{23}$ ;  $c_6=-c_1*K$ ;  $c_7=\omega_o*R_{fd}/X_{ad}$ ;  $Y_{11}=Y(1,1)$ ;  $c_8=-\omega_o*R_{fd}*Y_{11}$ ;  $Y_{12}=Y(1,2)$ ;  $c_9=-\omega_o*R_{fd}*Y_{12}$ ;  $Y_{13}=Y(1,3)$ ;  $V_b=0.932$ ;  $c_{10}=-\omega_o*R_{fd}*Y_{13}$ ;  $c_{11}=\omega_o*V_b$ ;  $c_{12}=\omega_o*(R_a)*Y_{21}$ ;

$c_{13}=\omega_o*(R_a)*Y_{22}$ ;  $c_{14}=\omega_o*(R_a)*Y_{23}$ ;  $Y_{31}=Y(3,1)$ ;

$c_{15}=-\omega_o*R_{kd}*Y_{31}$ ;  $c_{16}=-\omega_o*R_{kd}*Y(3,2)$ ;  $c_{17}=-\omega_o*R_{kd}*Y(3,3)$ ;

$c_{18}=\omega_o*(R_a)*D(1,1)$ ;  $c_{19}=\omega_o*(R_a)*D(1,2)$ ;

$c_{20}=-\omega_o*R_{kd}*D(2,1)$ ;  $c_{21}=-\omega_o*R_{kd}*D(2,2)$ ;

## References

- [1]. Andreev, M., Borovikov, Y., Gusev, A., Sulaymanov, A., Ruban, N., Suvorov, A., ... & Králík, T. (2018) Application of hybrid real-time power system simulator for research and setting a momentary and sustained fast turbine valving control. *IET Gener. Transm. Distrib.*, 12(1): 133-141.



- [2]. Franck, C. M. (2011). HVDC circuit breakers: A review identifying future research needs. *IEEE Transactions on Power Delivery*, 26(2): 998-1007.
- [3]. Øyvang, T., Hegglid, G. J., & Lie, B. (2018). Models of synchronous generators with excitation system, for transient power system studies. *IFAC-PapersOnLine*, 51(2):91-96.
- [4]. Bartlett, J. P., Gibbard, M. J., & Woodward, J. L. (1973, October). Performance of a 5 kVA synchronous generator with an optimal excitation regulator. In *Proceedings of the Institution of Electrical Engineers IET Digital Library*, Vol. 120(10) : 1250-1256.
- [5]. Franklin, G. F., Powell, J. D., & Workman, M. L. (1998). *Digital control of dynamic systems* (Vol. 3). Menlo Park, CA: Addison-wesley.
- [6]. Wang, Z., & Lemmon, M. (2016, July). Using decentralized secondary controllers to improve transient stability of generators in lossy power networks. In *American Control Conference (ACC)IEEE*: 5903-5908.
- [7]. Nazaruddin, Y. Y., & Unbehauen, H. (1996). Design of a multivariable state-space adaptive controller, and its application to a turbogenerator pilot plant. *Control Engineering Practice*, 4(5): 699-704.
- [8]. Sharaf, M. M., & Hogg, B. W. (1980). Identification and control of a laboratory model turbogenerator. *International Journal of Control*, 31(4):723-739.
- [9]. Sharaf, S. M., & Serag, A. M. (1995). Practical identification and PI optimal controller of a laboratory drive system. *International Journal of Control*, 62(3):511-526.
- [10]. Salgado, I., Mera, M., & Chairez, I. (2018). Suboptimal adaptive control of dynamic systems with state constraints based on Barrier Lyapunov functions. *IET Control Theory & Applications*, 12(8): 1116-1124.
- [11]. Venayagamoorthy, G. K., Harley, R. G., & Wunsch, D. C. (2002). Comparison of heuristic dynamic programming and dual heuristic programming adaptive critics for neurocontrol of a turbogenerator. *IEEE Transactions on Neural Networks*, 13(3): 764-773.
- [12]. Elsis, M., Soliman, M., Aboelela, M. A., & Mansour, W. (2017). Model predictive control of plug-in hybrid electric vehicles for frequency regulation in a smart grid. *IET Generation, Transmission & Distribution*, 11(16):3974-3983.
- [13]. Ersdal, A. M., Imsland, L., & Uhlen, K. (2016). Model predictive load-frequency control. *IEEE Transactions on Power Systems*, 31(1): 777-785.
- [14]. Elsis, M., Soliman, M., Aboelela, M. A. S., & Mansour, W. (2018). Improving the grid frequency by optimal design of model predictive control with energy storage devices. *Optimal Control Applications and Methods*, 39(1): 263-280.
- [15]. Venkat, A. N., Hiskens, I. A., Rawlings, J. B., & Wright, S. J. (2008). Distributed MPC strategies with application to power system automatic generation control. *IEEE transactions on control systems technology*, 16(6):1192-1206.
- [16]. Mohamed, T. H., Bevrani, H., Hassan, A. A., & Hiyama, T. (2011). Decentralized model predictive based load frequency control in an interconnected power system. *Energy Conversion and Management*, 52(2): 1208-1214.
- [17]. Maciejowski, J. M. (2002). *Predictive control with constraints*. Prentice Hall.
- [18]. Beielstein, T., Parsopoulos, K. E., & Vrahatis, M. N. (2002). Tuning PSO parameters through sensitivity analysis. Technical Report of the Collaborative Research Center 531 Computational Intelligence CI--124/02, University of Dortmund.
- [19]. Tavakoli, S., & Banookh, A. (2010). Robust PI control design using particle swarm optimization. arXiv preprint arXiv:1006-2805.
- [20]. Bartz-Beielstein, T., Parsopoulos, K. E., & Vrahatis, M. N. (2004, January). Analysis of particle swarm optimization using computational statistics. In *Proceedings of the International Conference of Numerical Analysis and Applied Mathematics ICNAAM 2004*: 34-37.
- [21]. Zhao, J., Li, T., & Qian, J. (2005, August). Application of particle swarm optimization algorithm on robust PID controller tuning. In *International Conference on Natural Computation*: 948-957. Springer, Berlin, Heidelberg.



- [22]. Solihin, M. I., Tack, L. F., & Kean, M. L. (2011). Tuning of PID controller using particle swarm optimization (PSO). *International Journal on Advanced Science, Engineering and Information Technology*, 1(4): 458-461.
- [23]. Giriraj Kumar, S. M., Sivasankar, R., Radhakrishnan, T. K., Dharmalingam, V., & Anantharaman, N. (2008). Particle swarm optimization technique based design of Pi controller for a real-time non-linear process. *Instrumentation Science and Technology*, 36(5): 525-542.
- [24]. Michon, M., Calverley, S. D., Clark, R. E., Howe, D., Chambers, J. D. A., Sykes, P. A., ... & Morris, G. (2007, September). Modelling and testing of a turbo-generator system for exhaust gas energy recovery. *In Vehicle Power and Propulsion Conference VPPC IEEE*: 544-550.
- [25]. Mai Hassan Hussein (2010). Fuzzy Neural Network for Control of Turbo-generator System. Master of Science Thesis, Faculty of Engineering, Helwan University.

